

Article

Parametrization of Fluid Models for Electrical Breakdown of Nitrogen at Atmospheric Pressure

Shirshak Kumar Dhali

Department of Electrical and Computer Engineering, Old Dominion University, Norfolk, VA 23320, USA; sdhali@odu.edu

Abstract: In the transient phase of an atmospheric pressure discharge, the avalanche turns into a streamer discharge with time. Hydrodynamic fluid models are frequently used to describe the formation and propagation of streamers, where charge particle transport is dominated by the creation of space charge. The required electron transport data and rate coefficients for the fluid model are parameterized using the local mean energy approximation (LMEA) and the local field approximation (LFA). In atmospheric pressure applications, the excited species produced in the electrical discharge determine the subsequent conversion chemistry. We performed the fluid model simulation of streamers in nitrogen gas at atmospheric pressure using three different parametrizations for transport and electron excitation rate data. We present the spatial and temporal development of several macroscopic properties such as electron density and energy, and the electric field during the transient phase. The species production efficiency, which is important to understand the efficacy of any application of non-thermal plasmas, is also obtained for the three different parametrizations. Our results suggest that at atmospheric pressure, all three schemes predicted essentially the same macroscopic properties. Therefore, a lower-order method such as LFA, which does not require the solution of the energy conservation equation, should be adequate to determine streamer macroscopic properties to inform most plasma-assisted applications of nitrogen-containing gases at atmospheric pressure.

Citation: Dhali, S.K. Parametrization of Fluid Models for Electrical Breakdown of Nitrogen at Atmospheric Pressure. *Plasma* **2024**, *7*, 721–732. <https://doi.org/10.3390/plasma7030037>

Academic Editors: Andrey Starikovskiy, Dariusz Z. Korzec and Maik Froehlich

Received: 9 July 2024

Revised: 2 August 2024

Accepted: 3 September 2024

Published: 10 September 2024



Copyright: © 2024 by the author. Licensee MDPI, Basel, Switzerland. This article is an open access article distributed under the terms and conditions of the Creative Commons Attribution (CC BY) license (<https://creativecommons.org/licenses/by/4.0/>).

1. Introduction

The development of an electrical discharge and the subsequent plasma formation is strongly dependent on the operating pressure and gas composition. Non-thermal plasmas, including low-pressure DC glows, RF discharges, and atmospheric pressure discharges, have many applications and serve as enabling technology in critical manufacturing processes [1–5]. The transient phase of an atmospheric pressure discharge consists of an avalanche that leads to the streamer phase. If left uninterrupted, it will eventually lead to an arc formation [6]. In most applications, the discharge is terminated: In repetitive nano-second pulse discharges, the pulse widths are short enough to avoid arc formation, and in dielectric barrier discharges, the charging of the dielectric quenches the micro discharge. From the perspective of plasma chemistry applications in such diverse areas as plasma medicine and plasma-assisted combustion, the understanding of reactive species production during the streamer phase is important [7,8]. The applications of non-thermal plasmas are based on the production of excited species, photo emission, and reactive radicals at or near ambient temperature [9–12]. These types of plasma are partially ionized gases, where the free electrons and heavy ions gain energy from the electric field and undergo elastic or inelastic collision with background particles or walls, leading to energy loss. Due to the large difference in the mass ratio, most of the energy gain from the field

is by electron transport across potential gradients. In certain applications with a changing gas composition, a computationally efficient model for the streamer development will help the implementation of complex plasma chemistry phenomena such as repetitively pulsed plasma-assisted combustion [7].

Non-thermal plasmas can reach a steady state in discharges, such as low-pressure DC glows or radio-frequency discharges, and others are classed as transient discharges, such as an atmospheric pressure streamer discharge. Near atmospheric pressure, electrical discharges produce spatially and temporally varying space charges that substantially alter the applied electric field and impose constraints on numerical models due to sharp spatial gradients. Non-local electron kinetics play an important role in low-pressure capacitively coupled RF discharge and low-pressure DC glows. We are particularly interested in studying the breakdown of atmospheric pressure gases. Non-thermal or cold plasma at atmospheric pressure forms the basis for many applications, including manufacturing, plasma medicine, disinfection, etc. [1,2,12].

The streamer mechanism was first proposed by Raether [13] and Leob and Meek [14] to explain electrical breakdown at high pressures. Since then, a large number of both experimental and numerical studies have resulted in a better understanding of its formation and propagation [15–23]. Theoretical efforts are constrained by the fact that the mathematical description of space charge-dominated transport is difficult to deal with because of the sharp density and field gradients. Most approaches to the modeling of streamers can be lumped under kinetic or fluid approaches. In kinetic models, the Boltzmann equation, coupled with the Poisson equation, is solved for the phase space of electrons. Alternatively, Monte Carlo simulations with a detailed particle transport using collisional cross-sections are used to determine the particle phase space. To cover the full six-dimensional phase space is computationally expensive, and this approach has found very little use in general. A computationally tractable hybrid approach is particle-in-cell Monte Carlo simulations (PIC-MCCs), where a large number of electrons are followed in the phase space using Monte Carlo techniques used to simulate collisions, and the electric field is obtained from the solution of Poisson's equation from the charged particle densities lumped in an appropriate mesh [21]. The 3-D PIC-MCCs have been particularly successful in modeling stochastic fluctuations, leading to the branching of streamers being observed experimentally [18]. Several articles have been published exploring the validity of the modeling approach for plasma fluid models: Nijdam et al. have reported numerical modeling including the pros and cons of the particle-in-cell (PIC) and fluid models [19]. Kim et al. benchmarked the PIC, fluid, and hybrids models by comparing simulation results with experimental results for plasma displays, capacitively coupled plasma, and inductively coupled plasma. They concluded that despite progress in the modeling and simulation of low-temperature plasma, these models still need improvements [20].

In plasma fluid models, the plasma hydrodynamics is described by macroscopic quantities such as electron density, drift velocity, and mean electron energy. The fluid models can be theoretically constructed by taking the velocity/energy moments of the Boltzmann equation. The first three moments give the particle, momentum, and energy conservation equations to describe the plasma hydrodynamics, and depending on the number of moments considered, appropriate closure approximations are required. The first-order drift-diffusion model based on local field approximation (LFA) has been used with some success in predicting and reproducing experimental results of the formation and propagation of streamer channels [15–23]. It has been reported that the assumption of local equilibrium of the electron energy deviates significantly at fast-changing ionization fronts with steep density and field gradients [19]. In the hydrodynamic description of non-thermal plasma, the electron transport and collisional rate coefficients are commonly parameterized by the local field or the local mean energy. For most commonly used gases, the transport and collision rates can be readily obtained from the two-term solution of the Boltzmann equation from electron impact cross-section data [24,25].

The second-order drift-diffusion model considers electron energy transport where the parameters are based on local mean energy approximation (LMEA), and several reports concluded that this model gives better results at streamer fronts. Luque and Ebert reviewed density models for streamer discharge simulation, detailing their physical foundation, their range of validity, and the most relevant algorithm employed in solving them [21]. Markosyan et al. compared plasma fluid models for one-dimensional streamer ionization fronts and compared them to the PIC model [22]. They found the local energy approximation and a higher-order model were in better agreement with the PIC simulations, and the local field approximation gave reasonably close results. Gruber et al. examined the local field and local energy models for the simulation of low-pressure DC glow and capacitively coupled RF discharges at low pressures (10 and 100 Pa) in argon and oxygen. They concluded that the LFA method is not recommended for gas discharge modeling in general at this pressure due to the inadequacy of the drift-diffusion approximation, and their results should be checked against experimental data or benchmark approaches [23].

We are interested in examining the plasma fluid models that would be suitable for investigating streamers near atmospheric pressures under ambient conditions. Although several publications have investigated this question, there are few results on the impact of the fluid model parametrization on excited species production. Our approach is not so much to replicate experimental results or streamer branching but come up with a suitable model to predict the important characteristics of a streamer that can inform the modeling of applications such as plasma medicine and plasma-assisted combustion. The purpose of the current paper is to understand under what condition are local field approximation and local mean energy approximation valid parameters for the transport and rate coefficients. In this paper, we simulate streamer development and propagation in nitrogen by using three different parametrization schemes and compare the important characteristics, such as excited species generation. Most applications are under ambient conditions; therefore, the study of nitrogen gas can serve as a good model.

2. Fluid Models for Streamer Discharges

During the transient phase, the heavy particles do not gain energy in this short period, and the neutral gas and ion are at or near room temperature. Also, in the time scale of interest (a few ns), the ions can be considered to be stationary compared to the lighter electrons. Both the first-order and the second-order fluid models for a non-attaching gas include the following particle conservation equations. In the first-order model, the parameter k is the local reduced electric field, E/N , and in the second-order model, it is the local mean electron energy, ε [15,22].

$$\frac{\partial n_e}{\partial t} = -\nabla \cdot \Gamma_e(k) + n_e \nu_I(k) + S \quad (1)$$

$$\frac{\partial n_i}{\partial t} = n_e \nu_I(k). \quad (2)$$

The quantity S represents various ion/electron source or sink mechanisms such as photoionization, recombination, attachment, or remnant space charge in repetitive discharges. In the absence of a magnetic field and assuming the velocity of the electrons is large compared to the slow species and the plasma is isothermal, the particle flux can be obtained from the momentum conservation equation and is given by [15,19]

$$\Gamma_e(\xi) = -n_e \mu_e(k) \mathbf{E} - D_e(k) \nabla n_e, \quad (3)$$

where n_e and n_i are the electron and positive ion density, respectively, μ_e is the electron mobility, D_e is electron diffusion coefficient, and ν_I is the ionization frequency.

In a slowly varying electric field where the magnetic field can be neglected, the electric field \mathbf{E} is obtained from the solution of the Poisson equation [15].

$$\begin{cases} \nabla^2 \phi = -q_e(n_i - n_e)/\epsilon_0, \\ \mathbf{E} = -\nabla \phi \end{cases} \quad (4)$$

where q_e is the unsigned electron charge and ϵ_0 is the free space permittivity.

In the second-order fluid model, the mean electron energy, ε , is determined from the energy conservation equation [22],

$$\frac{\partial n_e \varepsilon}{\partial t} = -\frac{5}{3} \nabla \cdot (\varepsilon \mathbf{E}) + q_e \mathbf{E} \cdot \mathbf{E} - n_e \sum_j k_j(\varepsilon) \epsilon_j, \quad (5)$$

where $k_j(\varepsilon)$ and ϵ_j are the electron energy-dependent collision rate coefficient and energy loss per electron per collision for the j^{th} collision process. The first term in the right-hand side of Equation (5) is the convective term, the second term is the energy gained from the electric field, and the third term is the energy loss due to inelastic collisions. This form of the energy conservation equation is derived by assuming the electron pressure tensor is isotropic [23]. A later part of this paper examines the contribution of each of these terms to the time evolution of the electron energy.

In streamer discharges, the ionization front propagates at speeds several times higher than the local drift velocity and experiences steep spatial gradients due to a rapid growth in ionization. It has been suggested that the first-order model is not adequate to describe the formation and propagation of these discharges, and a second-order model that calculates the local mean energy should be used [24]. The local mean energy can then be used as a parameter to estimate the transport parameters and rate coefficients.

In this article, three different parametrizations shown in Table 1 are investigated to understand the differences between the schemes in predicting streamer characteristics. The LMEA and the hybrid methods require the solution of the energy conservation equation. We introduce a new parameterization scheme (hybrid) where the mobility and diffusion are determined from the local electric field, which is readily available, and the electron impact rates such as ionization and excitation from the local electron energy. The justification for proposing this scheme is from a previous set of studies that show that the electron drift tracks the local electric field more closely compared to the electron energy [25].

Table 1. Parametrization schemes.

Local Field Approximation (LFA)	$\mu_e(\mathbf{E}/\mathbf{N})$, $D_e(\mathbf{E}/\mathbf{N})$	$\nu_I(\mathbf{E}/\mathbf{N})$	$k_j(\mathbf{E}/\mathbf{N})$
Local Mean Energy Approximation (LMEA)	$\mu_e(\varepsilon)$, $D_e(\varepsilon)$	$\nu_I(\varepsilon)$	$k_j(\varepsilon)$
Hybrid	$\mu_e(\mathbf{E}/\mathbf{N})$, $D_e(\mathbf{E}/\mathbf{N})$	$\nu_I(\varepsilon)$	$k_j(\varepsilon)$

3. Results and Discussion

The simulations were performed in two dimensions with azimuthal symmetry. The transport parameters and rate coefficients were determined using the open-source Boltzmann solver, BOLSIG+, with Lxcat nitrogen cross sections [26,27]. The Boltzmann solver solves for the electron energy distribution function for a given reduced electric field (\mathbf{E}/\mathbf{N}), which also provides the corresponding electron energy. The transport coefficients and rates can then be parameterized with either the reduced field or the electron energy.

The discharge consists of a gap of 5 mm filled with atmospheric-pressure nitrogen. The results presented here are for an applied step voltage of $V(t) = -25$ kV (186 Td), which resulted in an anode-directed streamer. The set of Equations (1)–(5) was solved numerically using the finite difference method. For all density variables, homogeneous Neumann boundary conditions, i.e., zero derivatives at the electrode boundaries, are prescribed [22]. A more physical boundary condition would require detailed knowledge of the electrode and secondary electrode processes. In such discharges, the cathode sheath has very little impact on the bulk properties of the streamer, which is of interest in most atmospheric pressure plasmas. The Flux-Corrected Transport (FCT) method proposed by Boris and Book was used for the convective term of both the electron density and electron

energy equations [28,29]. This method is particularly suitable for handling the steep density and field gradients encountered in streamer propagation. The contributions from the diffusion terms and from the impact ionization terms in Equation (1) were calculated at each time step and added to the convective term. The details can be found in reference [15]. A uniform grid spacing of 500 was used both in the z and r directions, giving a spatial resolution of 10 μm . The details of the method as applied to streamers have been extensively reported [15–17].

The following boundary conditions were used for the solution of the Poisson equation.

$$\left\{ \begin{array}{l} \phi = V(t) \text{ at } z = 0 \\ \phi = 0 \text{ at } z = 5 \text{ mm} \\ \frac{\partial \phi}{\partial t} = 0 \text{ at } r = 0 \\ \frac{\partial \phi}{\partial t} = 0 \text{ at } r = \infty \end{array} \right. . \quad (5)$$

The Poisson equation is solved for the electric potential by the Successive Over-Relaxation (SOR) method [3]. This is an iterative method and converges rapidly, as there is small perturbation from the previous time step. For our simulation, a relaxation factor $\omega = 1.9475$ gave the fastest convergence. The maximum relative error at any grid point was set to 10^{-5} for the convergence criterion.

The results presented here are for anode-directed streamers. The results were very similar for cathode-directed streamers. In order to bypass the avalanche phase, an initial neutral plasma is placed at the cathode, which represents the space charge formed. Details of this method and the background seeding of electrons to represent ionization can be found in references [15,16]. Figures 1–3 show the contour plots of electron density, electron energy, and electric field contours at different times for the fluid model with hybrid parametrization. These plots are typical of streamer propagation, where the streamer tip shows high gradients for electron density, electron energy, and electric field. In the streamer bulk, away from the tip, the electron energy and electric field is fairly constant.

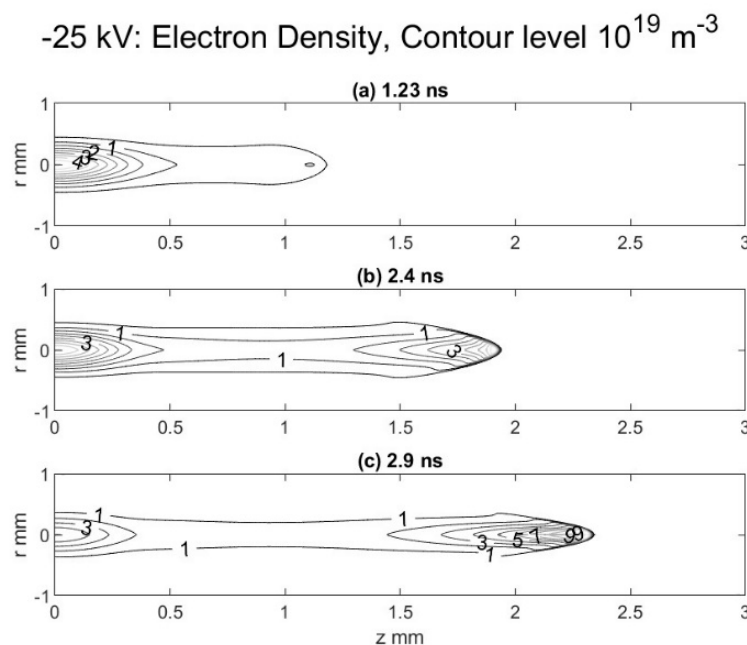


Figure 1. The contour plot of electron density at three different instances in time for nitrogen gas at one atmosphere for an applied voltage of 25 kV across a 5 mm gap. The z distance is from the cathode. The hybrid parametrization was used for the plasma model.

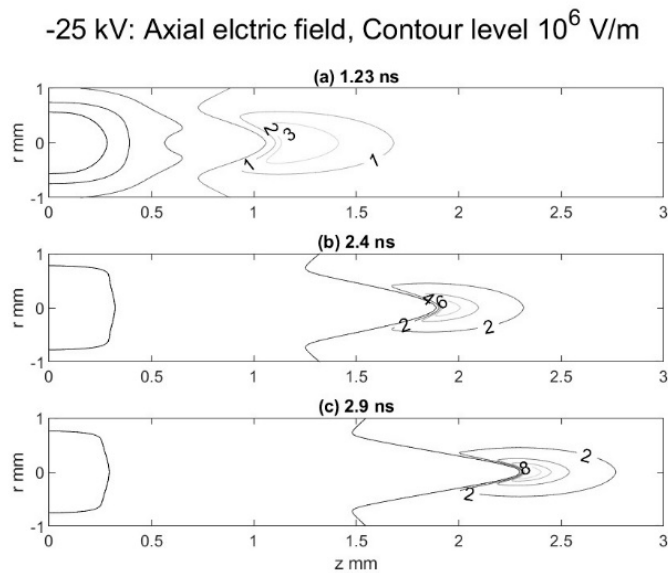


Figure 2. The contour plots of the axial electric field. All other conditions are the same as Figure 1.

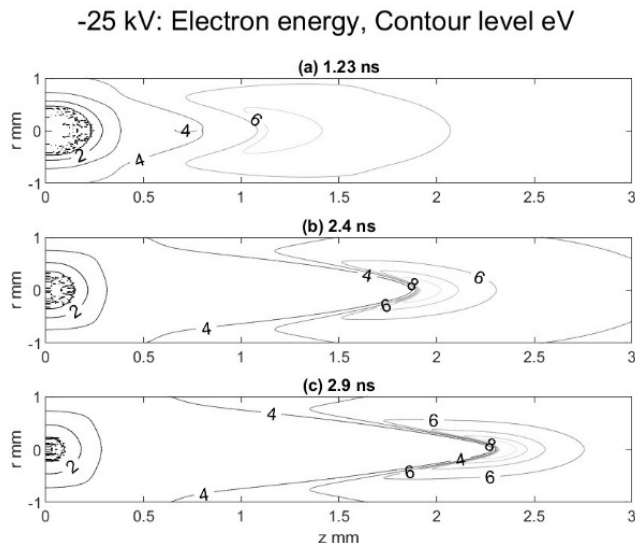


Figure 3. The on-axis plots of electron energy. All other conditions are the same as Figure 1.

The three different types of parametrizations result in similar contours plots. For comparison, the on-axis density and the electric field were plotted for streamer formation using the three different parametrizations at a nearly equal time and are shown in Figures 4 and 5, respectively. Since the time steps for the simulation are determined from the current Courant–Friedrichs–Lowy criteria, the comparison plots are not exactly at the same instant [30]. The electron density and the electric field as determined from three different parametrizations give very similar results with only a minor difference, which has very little impact on the development and propagation of the streamer.

The streamer speed as a function of time is shown in Figure 6 for the three different parametrizations. Again, we see very little difference in the speed, irrespective of the method used for solving the fluid equations. The speed of the ionization front increases with time, as the field enhancement at the tip of the streamer also increases with time as the streamer propagates. The higher the field enhancement, the quicker is the plasma density build-up due to electron impact ionization. The magnitude of the velocities of the streamer in nitrogen is close to experimentally reported values: Wagner reported an

anode-directed velocity of 0.4×10^6 m/s at 156 Td in atmospheric-pressure nitrogen, and Chalmers et al. reported an anode-directed velocity of 0.1 to 0.4×10^6 m/s in the range of 126 to 156 Td [31,32].

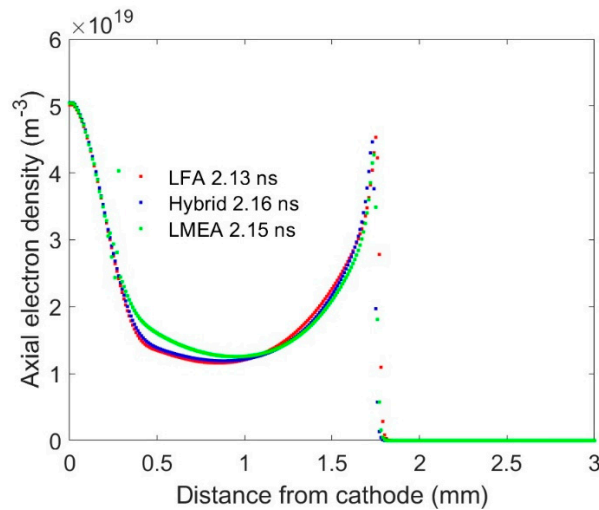


Figure 4. The axial electron density plots shown as a function of the distance from the cathode. The simulations conditions are the same as in Figure 1.

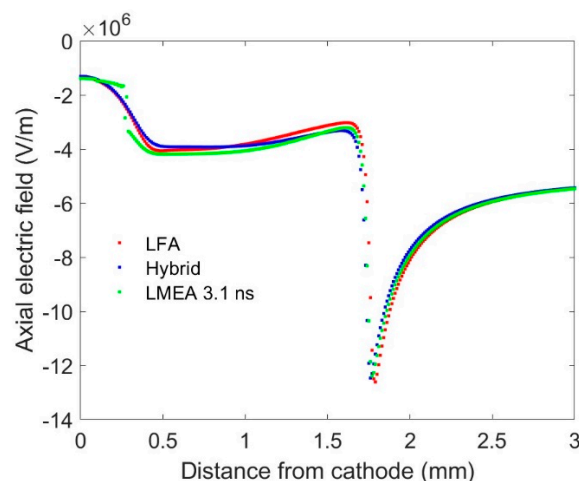


Figure 5. The on-axis electric field for the three different parametrizations. The simulations conditions are the same as in Figure 1.

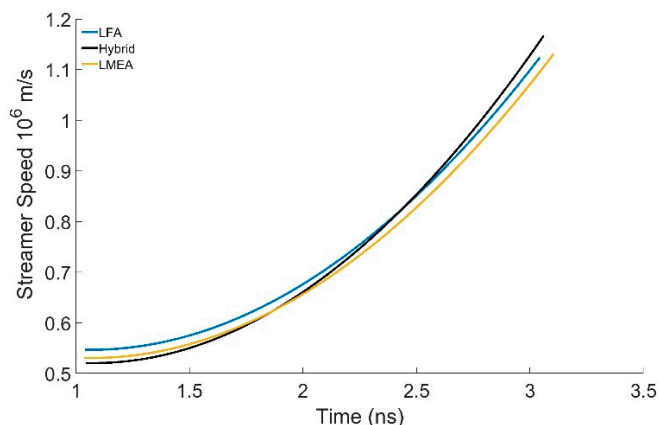


Figure 6. The streamer speed as a function of time from the start of the pulse for the three different parametrizations considered.

The spatial and temporal evolution of the energy obtained from the solution of the energy equation were compared to the energy predicted by the local electric field using the equilibrium relationship between the reduced electric field (E/N) in T_d and electron energy, ε , in nitrogen as obtained from the solution of the Boltzmann equation shown below.

$$\varepsilon = 0.924 + 0.0154(E/N) + 1.66 \times 10^{-5}(E/N)^2 + 7.8 \times 10^{-9}(E/N)^3 \text{ eV.} \quad (6)$$

The axial plot of the energy for the three different parameterizations is shown in Figures 7–9 for the LFA, hybrid, and LMEA, respectively. Remarkably, for all three parameterizations the electron energy agrees very well with the local electric field prediction at the streamer tip where the density and field gradients are the highest. There is a slight difference in the bulk of the streamer due to slight electron cooling predicted by the energy equation, which is discussed in a later section. The very steep rise in the electron density and the electric field in front of the streamer introduces some numerical oscillations, particularly in the later stages of the simulation. These oscillations will not have a significant impact in determining the excited species concentration.

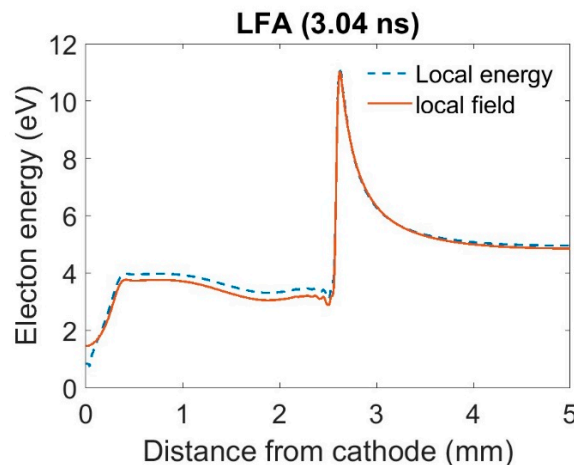


Figure 7. The on-axis electron energy as a function of the distance from the cathode determined from the energy equation (local energy) and the steady-state local field (Equation (7)) with LFA parametrization. The simulations conditions are the same as in Figure 1.

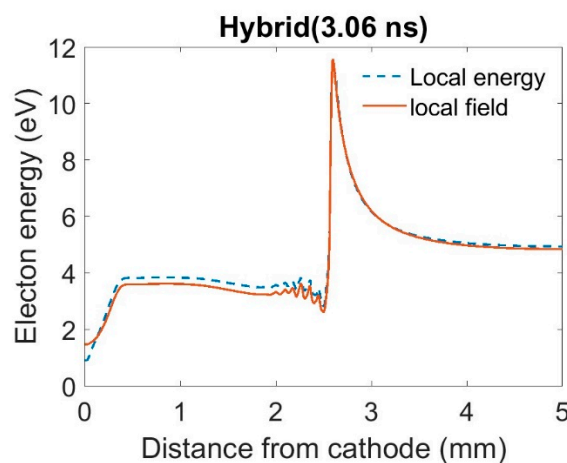


Figure 8. The on-axis electron energy as a function of the distance from the cathode determined from the energy equation (local energy) and the steady-state local field (Equation (7)) with hybrid parametrization. The simulations conditions are the same as in Figure 1.

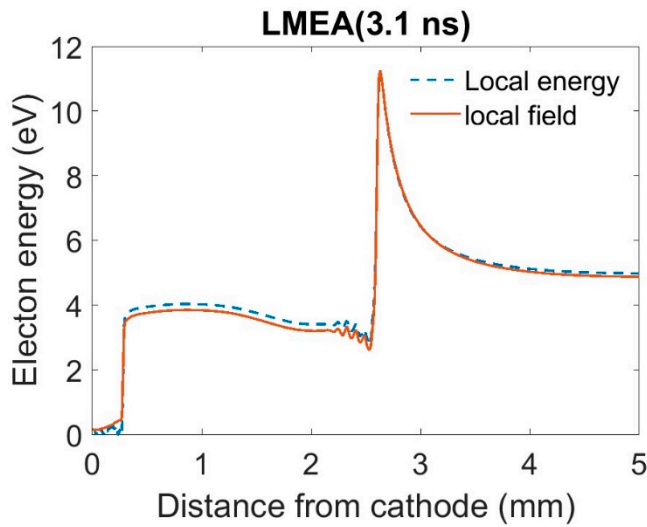


Figure 9. The on-axis electron energy as a function of the distance from the cathode determined from the energy equation (local energy) and the steady-state local field (Equation (7)) with LMEA parametrization. The simulations conditions are the same as in Figure 1.

In most applications where streamer-type discharges are used to generate excited species, an estimation of the species concentration is important in determining the subsequent plasma chemical pathways. Shown in Figure 10 is the G-factor, which is the number of radicals produced per 100 eV of electrical energy input, for three of the nitrogen excited states: $N_2(A^3\Sigma_u)$ (6.17 eV), $N_2(B^3\Pi_g)$ (7.35 eV), and $N_2(C^3\Pi_u)$ (11.03 eV) [33]. The three model parametrizations predict very similar G-factors, which remain fairly constant with time. The current increases with time as the streamer propagates along the axial direction. Therefore, the electrical energy input increases with time, and radical densities increase with time, although the G-factor does not change with time.

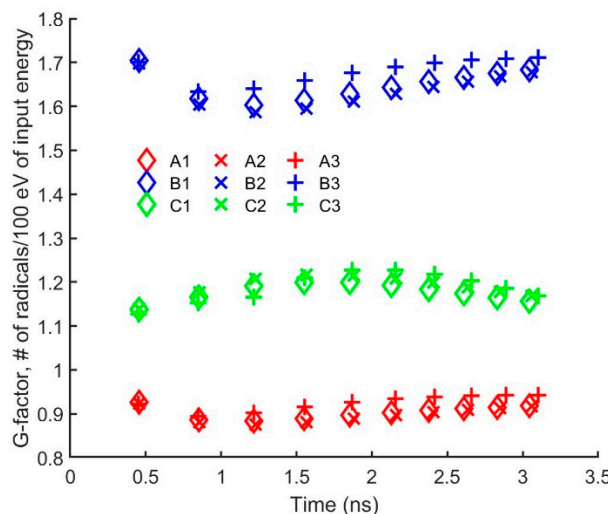


Figure 10. The G-factor (number of radicals produced per 100 eV of electrical energy) for three different nitrogen excited states as determined by the three different parametrization schemes: The \diamond , \times , and $+$ correspond to LFA, hybrid, and LMEA respectively, and red, blue, and green markers correspond to the $N_2(A^3\Sigma_u)$, $N_2(B^3\Pi_g)$, and $N_2(C^3\Pi_u)$ states, respectively.

The contribution to the energy change at spatial points along the axis was studied by looking at the first term on the right-hand side of the energy conservation equation, which is the convective term, and the net energy gain, which is the sum of the second (energy

gained from the electric field) and the third (energy lost due to inelastic process) terms. The energy gain from the electric field and the inelastic loss are almost equal and an order of magnitude higher than the convective contribution. Figure 11 shows the relative contribution due to the convective term, gain–loss term, and the net energy density rate for the hybrid and LMEA parametrizations. The LFA is not shown because the energy equation is not relevant to that method. At the streamer tip, there is a net transport of electron energy due to convection from the back to the front due to electron transport. The net effect is very similar in both parametrizations, and there is a net cooling behind the streamer tip. This cooling effect is seen in the energy plots (Figures 7–9) where the energy in the bulk shows a slight decline further away from the cathode.

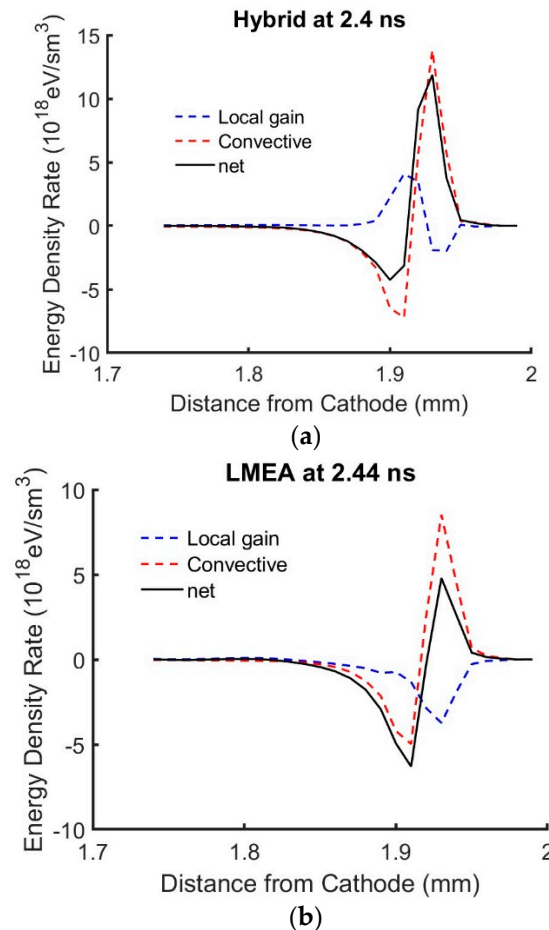


Figure 11. The contribution of convective and gain–loss terms in the energy equation. The solid black line is the net rate of energy density change at the spatial position in the axis. (a) The hybrid parametrization and (b) LMEA parametrization.

Our results suggest that the electron energy in a nitrogen streamer at atmospheric pressure quickly reaches equilibrium with the electric field, and the convective transport of energy does not have a significant impact. The various characteristics of the streamer discussed here show very little dependence on the parameterization. Markosyan et al. have performed similar studies in a 1-D streamer model. They compared different fluid models with a 1-D PIC simulation. Although the 1-D models have inherent shortcomings due to the gross simplification in estimating the spatial profile of the electric field, their findings are similar to what we observe in our simulations. A similar conclusion was reached by Wang et al., where they looked at particle and fluid models for streamer discharges in air [34]. Li et al. looked at the deviations from the LFA in negative streamer heads in nitrogen streamer heads when compared to particle models. They concluded that

the largest discrepancy is in the leading edge of the front where the electron density is very low, and the electric field is not screened [35]. As such, this result will have a minimum impact on estimating the overall radical generation in a streamer discharge. Our work confirms the choice of parametrization has very little impact on the species generation in the discharges studied.

4. Conclusions

At or near atmospheric pressure, the space charge-dominated transport of the streamer mechanism of the transient electrical breakdown of nitrogen was investigated using fluid models with three different parametrization schemes. These included the commonly known LEA and LMEA and a hybrid parametrization scheme, in which the drift and diffusion is determined from the local reduced electric field, and the electron impact rates are determined from the local electron energy. Several important characteristics of the streamer were reported, including electron density, electric field, electron energy, streamer velocity, and excited species production efficiency. These properties showed very little dependence on the parametrization scheme. We conclude that using a second-order method such as LMEA does not provide any additional advantage for high-pressure discharges in gases, such as air containing molecular gases like nitrogen, even in the presence of very steep density and field gradients. Our results suggest that the electron energy reaches local equilibrium, and the convective energy transport has a minimal impact on the overall electron energy. This conclusion is significant in developing efficient codes if the solution of the energy equation is required. For applications where repeated streamer simulation is required due to changing environments, this would save a considerable amount of computation time. It remains to be seen if this would apply for predominantly atomic gases that have a significantly different electron energy dependence on E/N due to the absence of energy loss to vibrational excitation.

Funding: This research was funded by by the US Office of Naval Research (Grant Number: W911NF-23-1-0173) and the National Science Foundation (Award Number: 2337461).

Institutional Review Board Statement: Not applicable

Informed Consent Statement: Not applicable

Data Availability Statement: The data that support the findings of this study are openly available in Refs. [25,26].

Conflicts of Interest: The authors declare no conflict of interest.

References

1. Kogelschatz, U. Dielectric-Barrier Discharges: Their History, Discharge Physics and Industrial Applications. *Plasma Chem. Plasma Process.* **2003**, *23*, 1.
2. Weltmann, K.D.; Kolb, J.F.; Holub, M.; Uhrlandt, D.; Simek, M.; Ostríkov, K.; Hamaguchi, S.; Cvelbar, U.; Cernak, M.; Locke, B.; et al. Future trends in plasma science and technology. *Plasma Process Polym.* **2009**, *16*, e1800118.
3. Li, J.; Sun W.; Pashaie, B.; Dhali, S.K. Streamer Discharge Simulation in Flue Gas. *IEEE Tran. Plasma Sci.* **1995**, *23*, 672.
4. Marode, E.; Goldman, A.; Goldman, M. Non-thermal plasma techniques for pollution control, Part A: Overview. In *Fundamentals and Supporting Technologies*; Penetrante, B.M., Schultheis, S.E., Eds.; NATO ASI Series; Springer: Berlin/Heidelberg, Germany, 1993; p. 167.
5. Dhali, S.K.) Generation of excited species in a streamer discharge. *AIP Adv.* **2021**, *11*, 015247.
6. Ganesh, S.; Rajaboshanam, A.; Dhali, S.K. Numerical Studies of Streamer to Arc Transition. *J. Appl. Phys.* **1992**, *72*, 9.
7. Adamovich, I.V.; Lempert, W.R. Plasma assisted ignition and high-speed flow control: Non-thermal and thermal effects. *Plasma Phys. Control. Fusion* **2015**, *57*, 01400.
8. Lu, X.P.; Reuter, S.; Laroussi, M.; Liu, D.W. *Nonequilibrium Atmospheric Pressure Plasma Jets: Fundamentals, Diagnostics, and Medical Applications*; CRC Press: Boca Raton, FL, USA, 2019; ISBN 978-0-429-62072-0.
9. Dhali, S.K. Generation of Large Volume Plasma using spatially and temporally rotating electric fields. *AIP Adv.* **2020**, *10*, 035002.
10. Sankaranarayanan, R.; Pashaie, B.; Dhali, S.K. Laser-Induced Fluorescence of OH Radicals in a dielectric-barrier discharge. *Appl. Phys. Lett.* **2000**, *77*, 2970.
11. Shakir, S.; Mynampati, S.; Pashaie, B.; Dhali, S.K. rf-generated ambient-afterglow plasma. *J. Appl. Phys.* **2006**, *99*, 073303.

12. Bruggeman, J.P.; Iza, F.; Brandenburg, R. Foundations of atmospheric pressure non-equilibrium plasmas. *Plasma Sources Sci. Technol.* **2017**, *26*, 123002.
13. Meek, J. M. Theory of spark discharge. *Phys. Rev.* **1940**, *57*, 722.
14. Loeb, J.B.; Meek, J.M. The mechanism of spark discharge in air at atmospheric pressure. *J. Appl. Phys.* **1940**, *11*, 438.
15. Dhali, S.K.; Williams, P.F. Two-dimensional Studies of Streamers in Gases. *J. Appl. Phys.* **1987**, *62*, 4696.
16. Dhali, S.K.; Pal, A.K. Numerical Simulation of Streamers in SF₆. *J. Appl. Phys.* **1987**, *63*, 1355.
17. Morrow, R. Theory of negative corona in oxygen. *Phys. Rev. A* **1985**, *32*, 1799.
18. Teunissen, J.; Ebert, U. 3D PIC-MCC simulations of discharge inception around a sharp anode in nitrogen/oxygen mixtures. *Plasma Sources Sci. Technol.* **2016**, *26*, 044005.
19. Nijdam, S.; Teunissen, J.; Ebert, U. The physics of streamer discharge phenomenon. *Plasma Sources Sci. Technol.* **2020**, *29*, 103001.
20. Kim, H.C.; Iza, F.; Yang, S.S.; Radmilovic-Radjenovic, M.; Lee, J.K. Particle and fluid simulations of low temperature plasma. *J. Phys. D: Appl. Phys.* **2005**, *38*, R283–R301.
21. Luque, A.; Ebert, U.J. Density models for streamer discharge, *Journal of Computational Physics*. *Comput. Phys.* **2012**, *231*, 904.
22. Markosyan, A.H.; Teunissen, J.; Dujko, S.; Ebert, U. Comparing plasma fluid models of different order for 1D streamer ionization fronts. *Plasma Sources Sci. Technol.* **2015**, *24*, 065002.
23. Bayle, P.; Cornebois, B. Propagation of ionizing electron shock waves in electrical breakdown. *Phys. Rev. A* **1985**, *31*, 1046–1058.
24. Grubert, G.K.; Becker, M.M.; Loffhagen, D. Why the local-mean-energy approximation should be used in hydrodynamic plasma descriptions instead of the local-field approximation. *Phys. Rev. E* **2009**, *80*, 036405.
25. Dhali, S.K. Transient behavior of drift and ionization in atmospheric nitrogen discharge. *Plasma Sources Sci. Technol.* **2022**, *31*, 025014. <https://doi.org/10.1088/1361-6595/ac43c6>.
26. Phelps Database. Available online: www.lxcat.net (accessed on 30 December 2020).
27. Hagelaar G.J.M.; Pitchford, L.C. Solving the Boltzmann equation to obtain electron transport coefficients for fluid models. *Plasma Source Sci. Technol.* **2005**, *14*, 722.
28. Zalesak, S.T. J. Fully Multidimensional flux-corrected transport algorithms for fluids. *Comput. Phys.* **1979**, *31*, 335.
29. Boris, J.P.; Book, D.L. Fluid transport algorithm that works. *Comput. Phys.* **1973**, *11*, 39.
30. Courant, R.; Friedrichs, K.; Lewy, H. On the partial difference equations of mathematical physic. *IBM J. Res. Dev.* **1967**, *11*, 215. <https://doi.org/10.1147/rd.112.0215>.
31. Wagner, K.H. Vorstudium des Funkens, untersucht mit dem Bildverstärker. *Z. Phys.* **1967**, *204*, 177.
32. Chalmers, I.D.; Duffy, H.; Tedford, D. J. The mechanism of spark breakdown in nitrogen, oxygen and sulphur hexafluoride. *Proc. R. Soc. Lond. A* **1972**, *329*, 171.
33. Lofthus, A.; Krupenie, P.H. The spectrum of molecular nitrogen. *J. Phys. Chem. Ref. Data* **1977**, *6*, 1.
34. Wang, Z.; Sun, A.; Teunissen, J. A comparison of particle and fluid models for positive streamer discharges in air. *Plasma Sources Sci. Technol.* **2021**, *31*, 015012.
35. Li, C.; Brok W. J. M.; Ebert, U.; Van der Mullen J. Deviation from the local field approximation in negative streamer heads. *J. Appl. Phys.* **2007**, *101*, 123305.

Disclaimer/Publisher’s Note: The statements, opinions and data contained in all publications are solely those of the individual author(s) and contributor(s) and not of MDPI and/or the editor(s). MDPI and/or the editor(s) disclaim responsibility for any injury to people or property resulting from any ideas, methods, instructions or products referred to in the content.